Insulating state to quantum Hall-like state transition in a spin-orbit-coupled two-dimensional electron system

Shun-Tsung Lo, Chang-Shun Hsu, Y. M. Lin, S.-D. Lin, C. P. Lee, Sheng-Han Ho, Chiashain Chuang, Yi-Ting Wang, and C.-T. Liang

Citation: Applied Physics Letters **105**, 012106 (2014); doi: 10.1063/1.4889847
View online: http://dx.doi.org/10.1063/1.4889847
View Table of Contents: http://scitation.aip.org/content/aip/journal/apl/105/1?ver=pdfcov
Published by the AIP Publishing

Insulating state to quantum Hall-like state transition in a spin-orbit-coupled two-dimensional electron system

Shun-Tsung Lo,[1,a)] Chang-Shun Hsu,[1,a)] Y. M. Lin,[2] S.-D. Lin,[2] C. P. Lee,[2] Sheng-Han Ho,[3] Chiashain Chuang,[3] Yi-Ting Wang,[3] and C.-T. Liang[1,3]
[1]*Graduate Institute of Applied Physics, National Taiwan University, Taipei 10617, Taiwan*
[2]*Department of Electronics Engineering and Institute of Electronics, National Chiao Tung University, Hsinchu 30010, Taiwan*
[3]*Department of Physics, National Taiwan University, Taipei 10617, Taiwan*

(Received 27 May 2014; accepted 23 June 2014; published online 9 July 2014)

We study interference and interactions in an InAs/InAsSb two-dimensional electron system. In such a system, spin-orbit interactions are shown to be strong, which result in weak antilocalization (WAL) and thereby positive magnetoresistance around zero magnetic field. After suppressing WAL by the magnetic field, we demonstrate that classical positive magnetoresistance due to spin-orbit coupling plays a role. With further increasing the magnetic field, the system undergoes a direct insulator-quantum Hall transition. By analyzing the magnetotransport behavior in different field regions, we show that both electron-electron interactions and spin-related effects are essential in understanding the observed direct transition. © *2014 AIP Publishing LLC*.
[http://dx.doi.org/10.1063/1.4889847]

The insulator-quantum Hall (I-QH) transition[1] is a fascinating physical phenomenon in the field of two-dimensional (2D) physics as it is related to the evolution of extended states between successive QH states with the magnetic field B. Experimentally, a temperature-independent point in the measured longitudinal resistivity ρ_{xx} of the 2D system at the crossing field B_c can be ascribed to evidence for the insulator-quantum Hall transition. For $B < B_c$, the 2D system behaves as an insulator in the sense that ρ_{xx} decreases with increasing temperature T.[2] For $B > B_c$, ρ_{xx} increases with increasing T, characteristics of a QH state.

Although in some cases the I-QH transition can be well described by the global phase diagram (GPD) developed by Kivelson, Lee, and Zhang,[1] a direct transition from an insulator to a high Landau-level filling factor $\nu > 2$ QH state which is normally described as the direct I-QH transition appears to be beyond the GPD. Such direct I-QH transitions have been observed in various systems such as SiGe hole gas,[2] GaAs multiple quantum well devices,[3] GaAs two-dimensional electron gases (2DEGs) containing InAs quantum dots,[4,5] a delta-doped GaAs quantum well with additional modulation doping,[6,7] GaN-based 2DEGs grown on sapphire[8] and on Si,[9] InAs-based 2DEGs,[10] and even some conventional GaAs-based 2DEGs,[11,12] suggesting that it is a universal effect. It is worth mentioning that the aforementioned results are obtained in spin-degenerate systems in which the spin effect and spin-orbit interactions are insignificant. Therefore, it is a fundamental issue whether the direct I-QH transition in a spin-orbit-coupled 2D system can occur, and it is the purpose of this paper to answer this important question. It is found here that the direct I-QH transition occurs with positive magnetoresistivity background. We show that electron-electron interactions, Zeeman splitting, and spin-orbit coupling play a role in describing the observed direct I-QH transition.

We have studied an InAs/InAsSb two-dimensional electron system (2DES). Such a device may find applications in narrow-gap material-based transistors and especially in spintronic devices owing to its strong spin-orbit coupling. The sample for this study was grown by a solid-source molecular beam epitaxy (MBE) system on a (001) semi-insulating GaAs substrate. The growth temperature was monitored by an infrared pyrometer. The As_2 and Sb_2 beams were controlled by cracker cells with needle valves, respectively. After a thermal cleaning at 600 °C ensured the removal of native oxides on the substrate, a GaAs buffer layer of 100 nm was grown at 580 °C to obtain a smooth surface. A relaxed metamorphic AlSb buffer layer of 1.3 μm grown at 520 °C was followed to accommodate the lattice mismatch between the active layers and the GaAs substrate. The active layers, from the bottom to the top, consist of a 4-nm-thick $AlAs_{0.16}Sb_{0.84}$ bottom barrier, a strained $InAs_{0.8}Sb_{0.2}$/InAs/$InAs_{0.8}Sb_{0.2}$ (3 nm/9 nm/3 nm) channel, and a 4-nm-thick $AlAs_{0.16}Sb_{0.84}$ layer. A 6-nm-thick AlSb top barrier and a 4-nm-thick highly lattice-mismatched $In_{0.5}Al_{0.5}As$ cap layer were then grown. The $In_{0.5}Al_{0.5}As$ layer keeps the underlying layers from oxidation. They were grown at 500 °C except the composite channel, which was grown at 470 °C. The carriers in the channel were provided by a Te delta-doped layer at the upper $AlAs_{0.16}Sb_{0.84}$/AlSb interface. Four-terminal magnetoresistivities were measured using standard ac phase-sensitive lock-in techniques. The magnetic field is applied perpendicular to the plane of the 2D electron system.

Figure 1 shows the longitudinal and Hall resistivities ρ_{xx} and ρ_{xy} as a function of magnetic field B at various T. There exists an approximately T-independent point in ρ_{xx} at $B_c = 0.73$ T. According to the low-field Hall effect, the carrier density is calculated to be $n = 1.43 \times 10^{16}\,m^{-2}$. We note that at the crossing point B_c, the corresponding Landau level filling factor is about 80 which is much bigger than 2. Therefore, we have observed a direct I-QH transition, consistent with existing experimental results.[2–12] We note

[a)]S.-T. Lo and C.-S. Hsu contributed equally to this work.

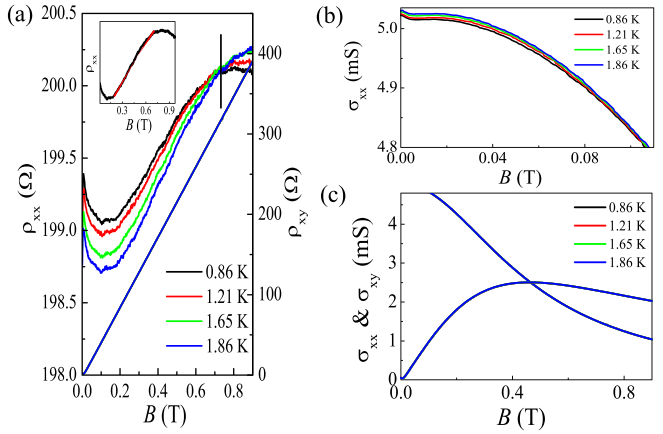

FIG. 1. (a) Longitudinal and Hall resistivities (ρ_{xx} and ρ_{xy}) as a function of magnetic field B at various temperatures T. The inset shows the fit to the data at $T = 0.86$ K using the two-band model from Ref. 32. (b) Longitudinal conductivity σ_{xx} (>4.8 mS) at various T. (c) Longitudinal and Hall conductivities (σ_{xx} and σ_{xy}) at various T.

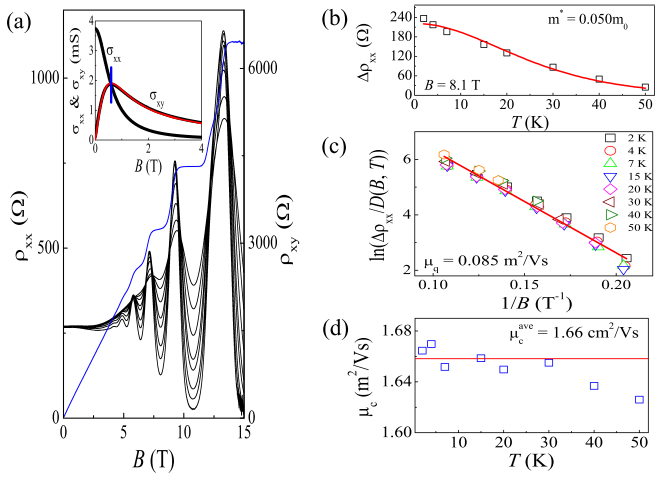

FIG. 3. (a) $\rho_{xx}(B)$ and $\rho_{xy}(B)$ at various T for $0 < B < 15$ T. From top to bottom at $B = 11$ T: $T = 50$, 40, 30, 20, 15, 7, 4, and 2 K. The inset shows $\sigma_{xx}(B)$ and $\sigma_{xy}(B)$ at $T = 1.966$ K together with the fit to σ_{xy} using the Drude model by Eq. (3). (b) The oscillating amplitude $\Delta\rho_{xx}(B = 8.1\,\text{T})$ as a function of T. The curve corresponds to the fit to the LK formula D(B, T). (c) Logarithm of $\Delta\rho_{xx}$ divided by $D(B, T)$ as a function of $1/B$. (d) The transport mobility determined from the fit shown in the inset of (a) as a function of T.

that the lack of change in the Hall slope as well as the non-vanishing ρ_{xx} suggest that a true QH state is not formed near B_c. Therefore, it is more appropriate to state that a direct transition from an insulating state to a quantum Hall-like state is seen. Figures 1(b) and 1(c) then show the longitudinal and Hall conductivities σ_{xx} and σ_{xy} as a function of magnetic field B obtained from $\rho_{xx}(B)$ and $\rho_{xy}(B)$ according to $\sigma_{xx}(B) = \rho_{xx}(B)/(\rho_{xx}(B)^2 + \rho_{xy}(B)^2)$ and $\sigma_{xy}(B) = \rho_{xy}(B)/(\rho_{xx}(B)^2 + \rho_{xy}(B)^2)$. It is found in Fig. 1(c) that σ_{xy} is T-independent over the whole range of $0 < B < 0.9$ T, suggesting that the carrier density does not vary with T. For $B > 0.1$ T, σ_{xx} is insensitive to the change in T. However, at low $B < 0.1$ T, σ_{xx} increases with increasing T as shown in Fig. 1(b). Such results are reminiscent of the quantum corrections caused by interference and interactions, both of which can give rise to a T dependence of σ_{xx}.

As shown in Fig. 1, for $0.1\,\text{T} < B < 0.75$ T, we see positive magnetoresistivity in the sense that ρ_{xx} increases with increasing B. In order to further study this effect as well as the observed direct I-QH transition, we have performed detailed low-field magneto-transport measurements. Such results are shown in Fig. 2(a). Positive magnetoresistivity centered at $B = 0$ is clearly observed. These experimental results are compelling evidence for weak anti-localization (WAL) due to spin-orbit coupling in two dimensions. As shown in Fig. 2(b), the converted magnetoconductivity $\Delta\sigma_{xx}(B) = \sigma_{xx}(B) - \sigma_{xx}(0)$ can be well fitted to conventional WAL theory.[13,14]

$$\Delta\sigma_{xx}(B) = \frac{e^2}{2\pi^2\hbar}\left\{\frac{3}{2}\Psi\left(\frac{1}{2}+\frac{B_2}{B}\right) - \Psi\left(\frac{1}{2}+\frac{B_1}{B}\right) - \frac{1}{2}\Psi\left(\frac{1}{2}+\frac{B_3}{B}\right) - \ln\left(\frac{{B_2}^{3/2}}{B_1 {B_3}^{1/2}}\right)\right\}, \quad (1)$$

with B_1, B_2, and B_3 as the fitting parameters, in which $\Psi(x)$ is the digamma function. The determined spin-orbit scattering time is approximately and T-independent. As shown in Fig. 2(c), the extracted phase coherence rate increases with increasing T. These results, together with the data shown in Fig. 1, clearly demonstrate that we have observed a direct I-QH transition in a spin-orbit-coupled two-dimensional electron system.

In the field of the direct I-QH transition, it is important to study important physical quantities such as the classical mobility, quantum mobility, and so on.[6,7,11,12] To this end, we have performed magneto-resistivity measurements to higher magnetic fields. Figure 3 shows ρ_{xx} and ρ_{xy} up to $B = 15$ T at various temperatures. Quantum Hall plateaus as well as Shubnikov-de Haas (SdH) oscillations are observed, demonstrating that we do have a two-dimensional system. It is known that the amplitudes of the SdH oscillations can be given by[15–17]

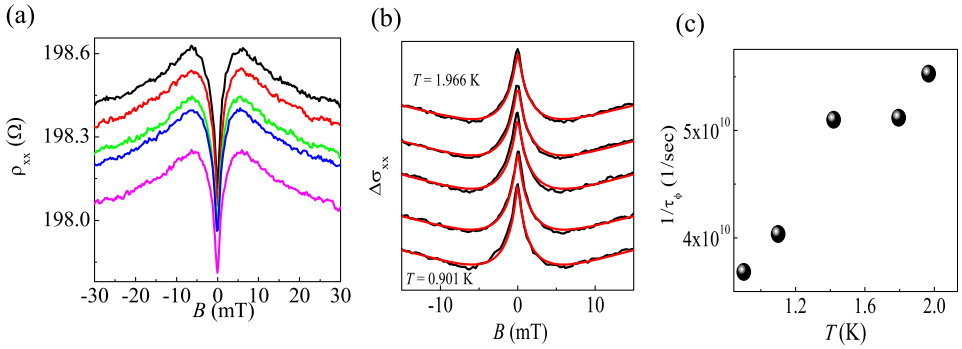

FIG. 2. (a) $\rho_{xx}(B)$ at various T showing weak antilocalization. From top to bottom: $T = 0.901$, 1.100, 1.420, 1.795, and 1.966 K. (b) Experimental data (in black) and fits to the data using Eq. (1) (in red). Curves have been vertically offset for clarity. (c) The determined phase coherence rate as a function of temperature.

$$\Delta\rho_{xx}(B,T) = c\exp(-\pi/\mu_q B)D(B,T), \quad (2)$$

where μ_q represents the quantum mobility, $D(B,T) = 2\pi^2 k_B m*T/\hbar eB\sinh(2\pi^2 k_B m*T/\hbar eB)$, and c is a constant relevant to the value of ρ_{xx} at $B = 0$ T. The effective mass is measured to be $0.050m_0$ from the thermal damping of SdH oscillation amplitude[15–17] at $B = 8.1$ T, where m_o is the rest mass of an electron, as shown in Fig. 3(b). In addition, the amplitudes of the SdH oscillations at various temperatures and magnetic fields allow us to calculate the quantum mobility μ_q to be 0.085 m^2/V s, which is presented in Fig. 3(c). By locating the oscillation extremes, one is able to obtain the carrier density $n = 1.43 \times 10^{16}\,m^{-2}$, consistent with the estimation from the low-field Hall measurements. On the other hand, the classical mobility μ_c is estimated to be 1.66 m^2/Vs by fitting the experimental $\sigma_{xy}(B)$ to the Drude $\sigma_{xy}(B) = ne\mu^2 B/(1+(\mu B)^2)$ as shown in the inset of Fig. 3(a). The obtained μ_c at various T is shown in Fig. 3(d). It is observed that μ_c is independent of T up to 30 K. A slight decrease of μ_c at $T > 30$ K is due to the influence of electron-phonon scattering. Since $\mu_c/\mu_q = 20$ which is much greater than 1, in our system the dominant scattering mechanism can be ascribed to remote ionized impurity scattering.[18] We note at the crossing point $\mu_c B_c = 1.2$–1, consistent with Huckestein's argument.[19] In contrast, the product $\mu_q B_c$ is about 0.06 which is significantly lower than 1. Our results on the direct I-QH transition obtained in a spin-orbit-coupled 2DES are consistent with those obtained in various conventional, spin-degenerate 2D system in the sense that $\mu_q B_c \ll 1$ and $\mu_c B_c \sim 1$.

In most cases, the direct I-QH transition occurs with negative magnetoresistivity background in the sense that around the crossing point ρ_{xx} decreases with increasing B. This can be understood within the following picture. Since the direct I-QH transition occurs when weak localization is suppressed at high magnetic fields. In this regime, negative magnetoresistivity which varies quadratically with B due to electron-electron interactions is generally observed. Interestingly, in our case, the observed direct I-QH occurs in the background of positive magnetoresistivity. Therefore, it is important to study this positive magnetoresistivity background. From the high-field magnetotransport data, we can estimate the transport relaxation time $\tau \approx 4.7 \times 10^{-13}$ s, mean free path $l \approx 3.3 \times 10^{-7}$ m, diffusion constant $D \approx 0.11$ m^2/s, and the Fermi wave vector $k_F \approx 3.0 \times 10^8\,m^{-1}$, which is required in the following analyses.

In our device $k_F l = 98$, demonstrating that our system is weakly disordered and hence validating the use of quantum correction theory for analyzing the data.[20–25] In the ballistic regime ($k_B T\tau/\hbar > 1$), electron-electron interactions may give rise to positive magnetoresistivity.[26,27] Moreover, the classical mobility would be renormalized by this ballistic-type interaction and thereby becomes T-dependent.[23,24] However, in our system $\hbar/(k\tau) \approx 16$ K and therefore for $T \ll 16$ K the observed positive magnetoresistivity in Fig. 1(a) cannot be due to electron-electron interactions in the ballistic regime. In Fig. 3(d), we know that the classical mobility μ_c is independent of T (<30 K). Therefore, our system is in the diffusive regime ($k_B T\tau/\hbar \ll 1$). It is predicted that the electron-electron interactions in the diffusive regime contributes to σ_{xx} only.[20,21] Since the classical Dude conductivities in the magnetic field have the form $\sigma^D_{xx}(B) = ne\mu_c/(1+(\mu_c B)^2)$ and $\sigma^D_{xy}(B) = ne\mu_c^2 B/(1+(\mu_c B)^2)$, the magnetoresistivity considering this type of interactions $\delta\sigma^{ee}_{xx}(T,B)$ is given as

$$\rho_{xx}(B) \approx \frac{1}{\sigma_0} - \frac{1}{\sigma_0^2}\left(1-\mu_c^2 B^2\right)\delta\sigma^{ee}_{xx}(T,B), \quad (3)$$

by performing matrix inversion of the conductivity tensor, where $\sigma_0 \equiv \sigma^D_{xx}(B=0)$.[21,22] When $g\mu_B B < k_B T$, where g is the Landé g-factor, μ_B is the Bohr magneton, the correction due to electron-electron interactions would become independent of B, that is, $\delta\sigma^{ee}_{xx}(T) = \frac{e^2}{2\pi^2\hbar}K_{ee}\ln\left(\frac{k_B T\tau}{\hbar}\right) < 0$ in Eq. (2), where the prefactor K_{ee} is approximately B-independent here.[21,22] Therefore, in GaAs-based 2D systems whose $g_{GaAs} \approx 0.44$ at low fields,[28] quadratic negative magnetoresistivity will exist for $T > 0.22$ K at B around 0.73 T. However, for InAs-based devices whose g can be as large as $10g_{GaAs}$,[29] Zeeman splitting could play a role at $B_c = 0.73$ T when $T < 2.2$ K, which covers the whole T range in our measurements shown in Fig. 1(a). We note that according to the theory of interactions in the diffusive regime, K_{ee} will increase with increasing the Zeeman splitting when $g\mu_B B > k_B T$,[20] which indicates that the resulting magnetoresistivity is still negative but deviates from the quadratic form. Therefore, Eq. (3) cannot provide good enough explanations for our data. Nevertheless, it should be noted that the theory is derived based on the short-range disorder.[30,31] In our case, long-range disorder predominates the system since $\mu_c/\mu_q = 20$. In addition, as will be shown later, a classical mechanism may lead to positive magnetoresistivity background, which can overwhelm the negative magnetoresistivity induced by interactions described by Eq. (3). We note that $B_{tr} \approx 3$ mT, within which the localization effect is strongest, Therefore, the observed T dependence of ρ_{xx} at $B > 0.13\,\text{T} \gg B_{tr}$ shown in Fig. 1(a) should still be ascribed to electron-electron interactions.

Since we have observed weak anti-localization due to spin-orbit coupling, we should consider the two-band model for two spin species. As shown in the inset of Fig. 1(a), our data can be well fitted by the two-band model developed by Zaremba,[32] where intersubband scattering is included. Therefore, the observed positive magnetoresistivity background can be ascribed to the two spin-split bands due to spin-orbit interactions. In InAs-based 2D systems, spin-orbit coupling and Zeeman effect are expected to be strong. Further experimental and theoretical work on the magnetotransport with the presence of electron-electron interactions[33] in such a system is highly required.

In conclusion, we present an experimental investigation of direct I-QH transition in a spin-orbit coupled 2D electron system. Instead of negative magnetoresistivity, we show that a direct I-QH transition can occur with positive magnetoresistivity background. By studying the conductivities at low fields and SdH oscillations at high fields, our results demonstrate that the observed transition in such a system is related to Zeeman splitting, spin-orbit coupling, and electron-electron interactions.

This work was funded by National Taiwan University (Grant No. 103R7552-2), and in part, by the Ministry of Science and Technology, Taiwan. We would like to thank Professor Xi Lin at PKU, China for discussions.

[1]S. Kivelson, D.-H. Lee, and S.-C. Zhang, Phys. Rev. B **46**, 2223 (1992).
[2]S. H. Song, D. Shahar, D. C. Tsui, Y. H. Xie, and D. Monroe, Phys. Rev. Lett. **78**, 2200 (1997).
[3]C. H. Lee, Y. H. Chang, Y. W. Suen, and H. H. Lin, Phys. Rev. B **56**, 15238 (1997).
[4]T.-Y. Huang, J. R. Juang, C. F. Huang, G.-H. Kim, C.-P. Huang, C. T. Liang, Y. H. Chang, Y. F. Chen, Y. Lee, and D. A. Ritchie, Physica E **22**, 240 (2004).
[5]T.-Y. Huang, C. T. Liang, G.-H. Kim, C. F. Huang, C.-P. Huang, J.-Y. Lin, H.-S. Goan, and D. A. Ritchie, Phys. Rev. B **78**, 113305 (2008).
[6]D.-S. Luo, L.-H. Lin, Y.-C. Su, Y.-T. Wang, Z. F. Peng, S.-T. Lo, K. Y. Chen, Y. H. Chang, J.-Y. Wu, Y. Lin, S.-D. Lin, J. C. Chen, C. F. Huang, and C.-T. Liang, Nanoscale Res. Lett. **6**, 139 (2011).
[7]S.-T. Lo, K. Y. Chen, T. L. Lin, L.-H. Lin, D.-S. Luo, Y. Ochiai, N. Aoki, Y.-T. Wang, Z. F. Peng, Y. Lin, J. C. Chen, S.-D. Lin, C. F. Huang, and C. T. Liang, Solid State Commun. **150**, 1902 (2010).
[8]J.-Y. Lin, J.-H. Chen, G.-H. Kim, H. Park, D. H. Youn, C. M. Jeon, J. M. Baik, J.-L. Lee, C.-T. Liang, and Y. F. Chen, J. Korean Phys. Soc. **49**, 1130 (2006).
[9]E. S. Kannan, G. H. Kim, J. Y. Lin, J. H. Chen, K. Y. Chen, Z. Y. Zhang, C.-T. Liang, L. H. Lin, D. H. Youn, K. Y. Kang, and N. C. Chen, J. Korean Phys. Soc. **50**, 1643 (2007).
[10]K. H. Gao, G. Yu, Y. M. Zhou, L. M. Wei, T. Lin, L. Y. Shang, L. Sun, R. Yang, W. Z. Zhou, N. Dai, J. H. Chu, D. G. Austing, Y. Gu, and Y. G. Zhang, J. Appl. Phys. **108**, 063701 (2010).
[11]S.-T. Lo, Y.-T. Wang, G. Bohra, E. Comfort, T. Y. Lin, M. G. Kang, G. Strasser, J. P. Bird, C. F. Huang, L.-H. Lin, J. C. Chen, and C. T. Liang, J. Phys.: Condens. Matter **24**, 405601 (2012).
[12]S.-T. Lo, Y.-T. Wang, S.-D. Lin, G. Strasser, J. P. Bird, Y.-F. Chen, and C.-T. Liang, Nanoscale Res. Lett. **8**, 307 (2013).
[13]S. Hikami, A. I. Larkin, and Y. Nagaoka, Prog. Theor. Phys. **63**, 707 (1980).
[14]M. Eshkol, E. Eisenberg, M. Karpovski, and A. Palevski, Phys. Rev. B **73**, 115318 (2006).
[15]A. B. Fowler, F. F. Fang, W. E. Howard, and P. J. Stiles, Phys. Rev. Lett. **16**, 901 (1966).
[16]P. T. Coleridge, R. Stoner, and R. Fletcher, Phys. Rev. B **39**, 1120 (1989).
[17]P. T. Coleridge, Semicond. Sci. Technol. **5**, 961 (1990).
[18]S. J. MacLeod, K. Chan, T. P. Martin, A. R. Hamilton, A. See, A. P. Micolich, M. Aagesen, and P. E. Lindelof, Phys. Rev. B **80**, 035310 (2009).
[19]B. Huckestein, Phys. Rev. Lett. **84**, 3141 (2000).
[20]G. M. Minkov, O. E. Rut, A. V. Germanenko, A. A. Sherstobitov, V. I. Shashkin, O. I. Khrykin, and V. M. Daniltsev, Phys. Rev. B **64**, 235327 (2001).
[21]G. M. Minkov, O. E. Rut, A. V. Germanenko, A. A. Sherstobitov, B. N. Zvonkov, E. A. Uskova, and A. A. Birukov, Phys. Rev. B **65**, 235322 (2002).
[22]G. M. Minkov, O. E. Rut, A. V. Germanenko, A. A. Sherstobitov, V. I. Shashkin, O. I. Khrykin, and B. N. Zvonkov, Phys. Rev. B **67**, 205306 (2003).
[23]G. M. Minkov, A. V. Germanenko, O. E. Rut, A. A. Sherstobitov, V. A. Larionova, A. K. Bakarov, and B. N. Zvonkov, Phys. Rev. B **74**, 045314 (2006).
[24]G. M. Minkov, A. V. Germanenko, O. E. Rut, A. A. Sherstobitov, and B. N. Zvonkov, Phys. Rev. B **76**, 165314 (2007).
[25]K. E. J. Goh, M. Y. Simmons, and A. R. Hamilton, Phys. Rev. B **77**, 235410 (2008).
[26]A. Y. Kuntsevich, G. M. Minkov, A. A. Sherstobitov, and V. M. Pudalov, Phys. Rev. B **79**, 205319 (2009).
[27]T. A. Sedrakyan and M. E. Raikh, Phys. Rev. Lett. **100**, 106806 (2008).
[28]T.-Y. Huang, C.-T. Liang, Y. F. Chen, M. Y. Simmons, G.-H. Kim, and D. A. Ritchie, Nanoscale Res. Lett. **8**, 138 (2013).
[29]G. Papp and F. M. Peeters, Appl. Phys. Lett. **78**, 2184 (2001).
[30]B. L. Altshuler and A. G. Aronov, *Electron-electron interactions in disordered systems*, edited by A. L. Efros and M. Pollak (North Holland, Amsterdam, 1985).
[31]G. Zala, B. N. Narozhny, and I. L. Aleiner, Phys. Rev. B **64**, 214204 (2001).
[32]E. Zaremba, Phys. Rev. B **45**, 14143 (1992).
[33]Y.-F. Lu, S.-T. Lo, J.-C. Lin, W. Zhang, J.-Y. Lu, F.-H. Liu, C.-M. Tseng, Y.-H. Lee, C.-T. Liang, and L.-J. Li, ACS Nano **7**, 6522 (2013).